• Around O and B stars, circumstellar HII regions exist in a **Strömgren sphere** about massive protostellar environments (*draw schematic*). The radius of this sphere directly couples to the stellar UV flux. The dynamical structure of such an HII region is controlled by the rate of recombination

$$\frac{dn_{\rm recom}}{dt} \;=\; \alpha n_e n_{\rm H} \;=\; \alpha n_{\rm H}^2 \tag{15}$$

in the intense UV bath. Here we have invoked charge neutrality $n_e = n_{\rm H}$, and α is the quantum mechanical recombination rate coefficient.

If dN_{UV}/dt is the rate of generation of UV photons by the central star then the HII sphere oblates until all UV photons are absorbed, defining a the Strömgren radius $R_{\rm S}$, outside of which there exists an HI region:

$$\alpha n_e n_{\rm H}\left(\frac{4\pi}{3}\,R_{\rm S}^3\right) \;=\; \frac{dN_{UV}}{dt} \;\equiv\; \frac{L_{UV}}{\langle\varepsilon_{UV}\rangle} \quad , \tag{16}$$

with $\langle\varepsilon_{UV}\rangle \gtrsim 13.6\,{\rm eV}$. This inverts to

$$R_{\rm S} \;=\; \left(\frac{3}{4\pi\alpha}\,\frac{dN_{UV}}{dt}\right)^{1/3} n_{\rm H}^{-2/3} \quad . \tag{17}$$

If one can measure $R_{\rm S}$ and the UV luminosity blue-ward of 13.6eV, then it becomes possible to infer $n_{\rm H}$ in Strömgren spheres.

• OB stars and HII regions tend to clump together in what we call **OB associations**, spawned by multiple cores in GMCs

Examples of well-formed pre-main sequence objects are **T-Tauri stars**, low mass protostars with very significant winds and associated mass loss.

• These exhibit evidence of expanding *thickish* winds via emission/absorption line diagnostics that reveal **P Cygni** profiles, which can be used for diagnostics on wind speed and shell column density of $n_{\rm H}$.

Plot: P Cygni Line Profile

• Protostellar objects possess angular momentum and are far from spherical. Often, T-Tauri stars possess jets and accretion disks ($\Rightarrow$ aspherical winds): these are called **Herbig-Haro objects**, first identified by Herbig and Haro.

Plot: Herbig-Haro Object Schematic

P Cygni Line Profile

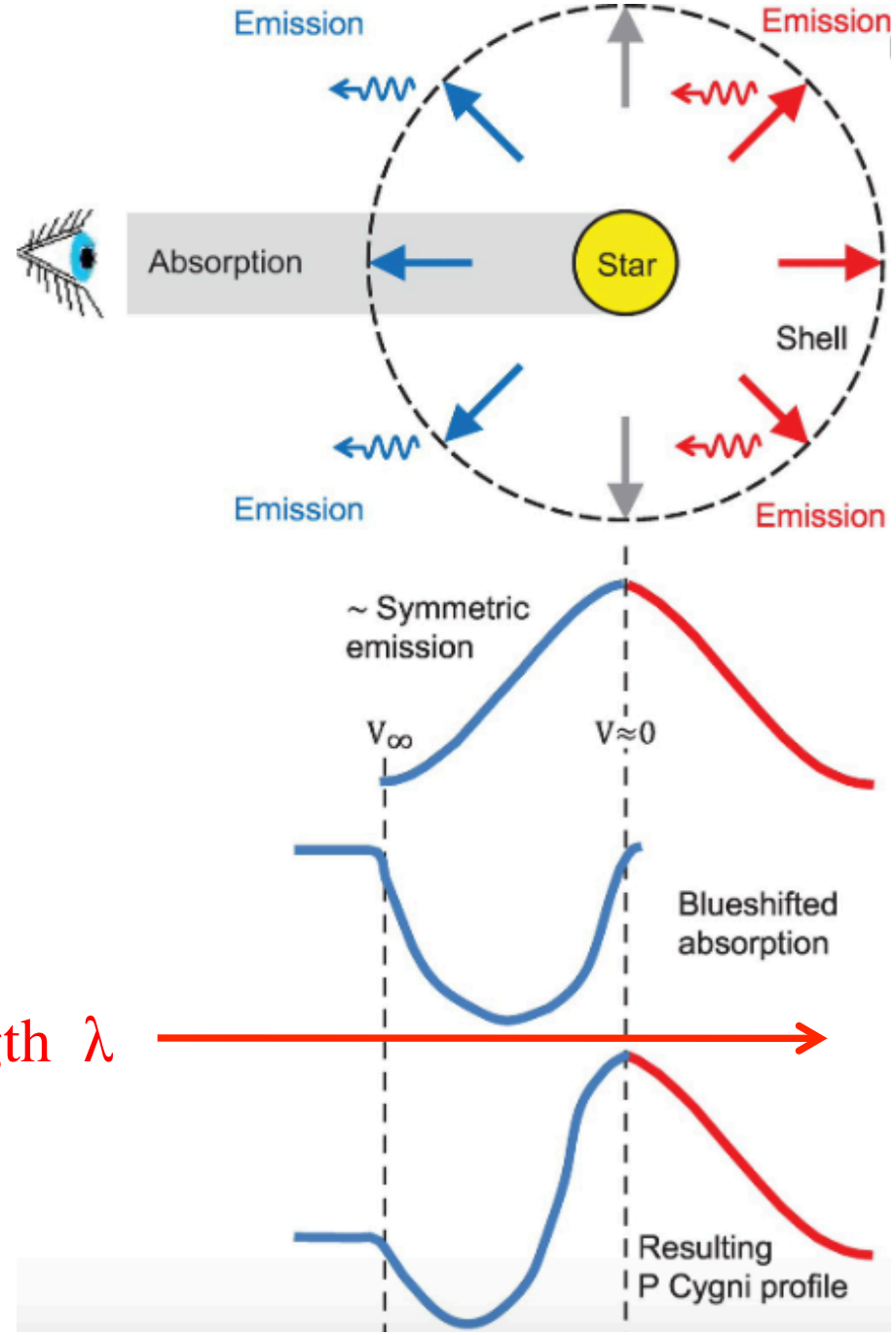

- Credit: R. Walker (LBV Stars, CUP)

Herbig-Haro Object

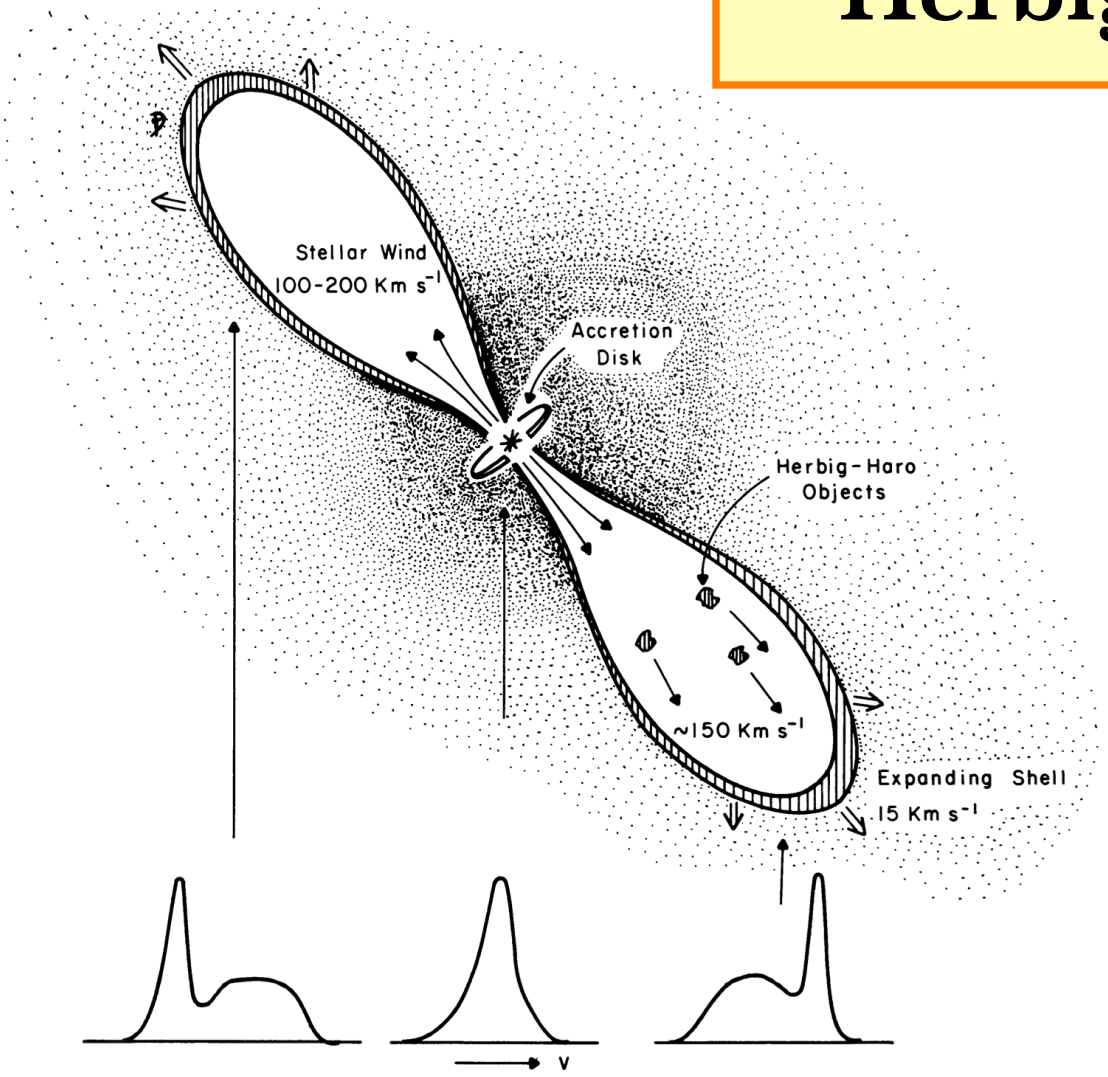

- A model of the T Tauri star in the molecular cloud L1551, with an accretion disk, and a collimated wind/jet named a Herbig-Haro Object.
- Snell, Loren & Plambeck (1980, ApJL 239, L17)

2 Evolution on the Main Sequence

The main sequence in the HR diagram is not a locus of zero thickness due to differing chemical compositions, stages of evolution of the stars, and also due to observational uncertainties. The sun is not quite a **zero age main sequence** (ZAMS) star, having evolved somewhat since birth. **C & O, Sec. 13.2**

• During this evolution, core hydrogen burning in the sun increases the mean molecular weight μ somewhat, reducing the pressure supporting gravity.

∗ The core radius R_c is reduced, $P_c \sim GM_c^2/R_c^4$ rises so that the core temperature T_c rises.

• This pushes the nucleosynthetic luminosity higher, though the energy supply is tapped to expand the stellar envelope to larger radii. Eventually, the inflation dominates the use of increased energy generation so that the star only maintains luminosity while dropping its effective temperature $T_{\rm eff}$.

∗ Accordingly, the solar luminosity increases, so that the radius and interior temperature increase, but the surface temperature $T_{\rm eff}$ declines.

∗ For more massive stars, the increase in radius is more profound.

Plot: Stellar Evolutionary Tracks on the HR Diagram

• For later stages of the evolution of a solar mass star, once core hydrogen is significantly depleted, the inner structure is a dense helium core with *a surrounding hydrogen-burning shell*. The shell actually burns at *a higher temperature* than the original hydrogen core, due to the new hydrostatic equilibrium involving an isothermal helium core.

∗ This portion of redward evolution on the HR diagram is called the **subgiant branch**. Its onset marks when the mass of the helium core is so great that it cannot support the material above it.

Plot: Gaia Hertzsprung-Russell Diagram for Open Clusters

Main Sequence Stellar Evolution

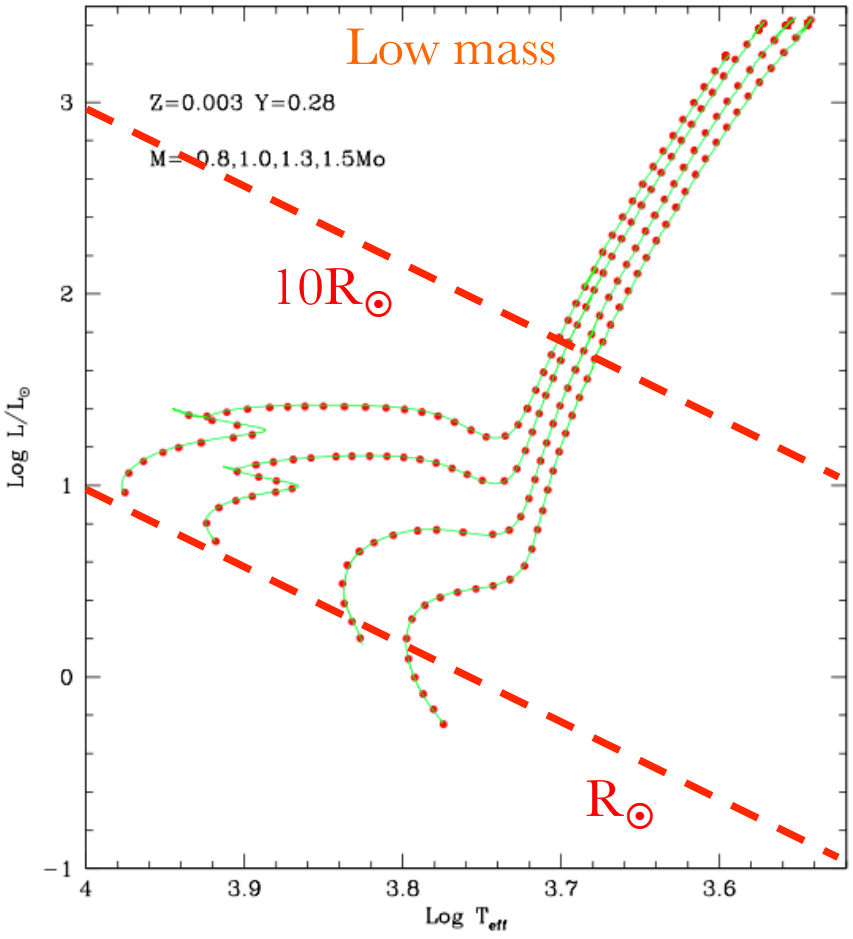

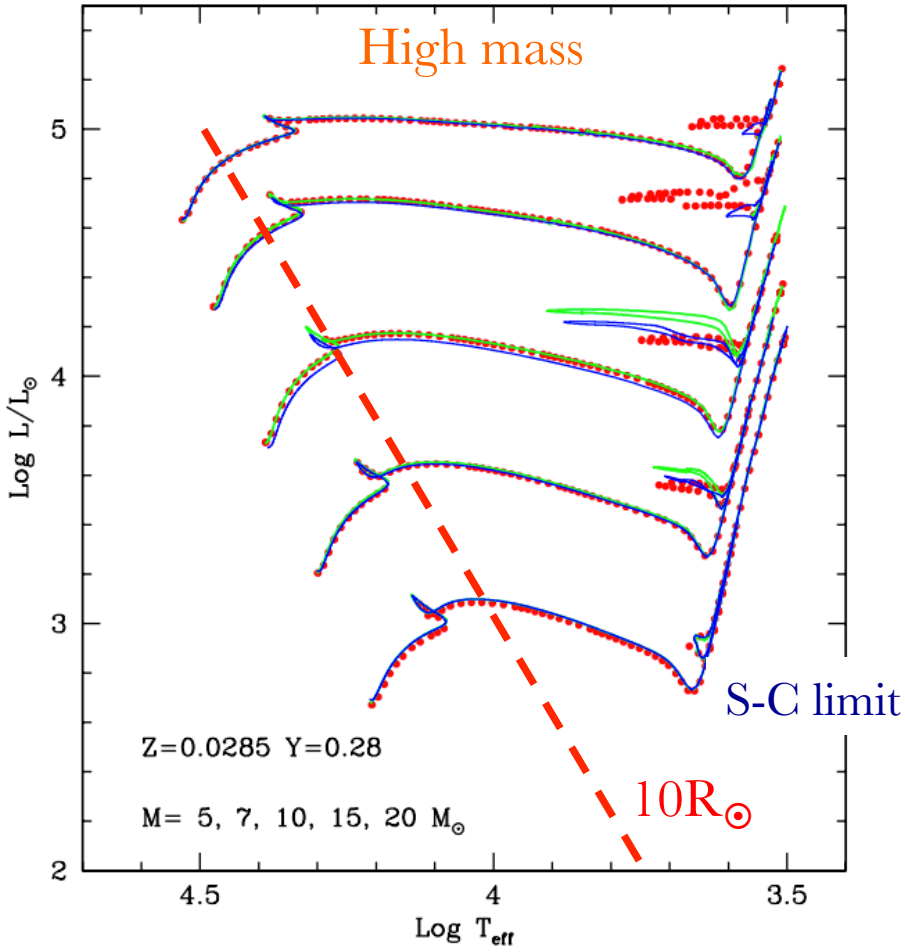

- *Left*: low mass stars. *Right*: high mass stars. Z=metallicity, Y = He mass fraction.
- From G. Bertelli et al., A&A (2008, **484**, 815; 2009, **508**, 355).

Gaia HR Diagram for Open Clusters

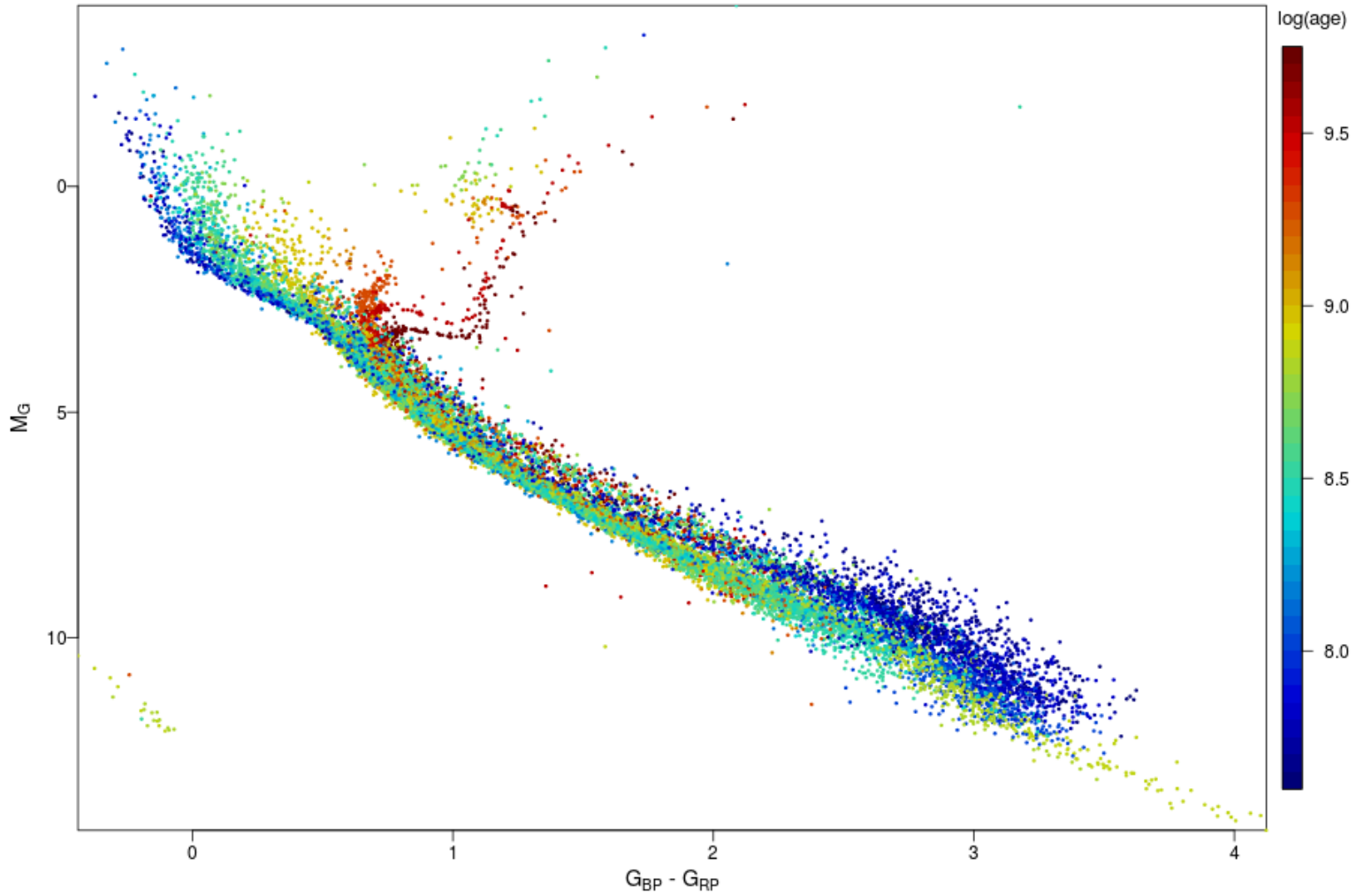

- Observational HR diagram from Gaia Data Release 2 (DR2) for 32 open clusters of main sequence and white dwarf stars. Cluster age is color-coded in years (log scale) according to bar on right. Babusiaux et al. A&A **616**, A10 (2018).

2.1 The Schönberg-Chandrasekhar Limit

• The mass of the isothermal core at the start of the subgiant branch can be simply related to the ratio of the mean molecular weights in the envelope (μ_e) and the core (μ_c), and is called the **Schönberg-Chandrasekhar limit**:

$$\frac{M_c}{M} \approx 0.37 \left(\frac{\mu_e}{\mu_c}\right)^2 \quad . \tag{18}$$

Carroll and Ostlie detail an estimation of this limit. Let us distill this as follows.

Plot: Sketch two-zone Structure in Sub-Giants

The stellar interior satisfies (longish derivation) a modified virial theorem:

$$4\pi R_c^3 P_c - 2K_c = U_c \quad , \tag{19}$$

where the core kinetic energy is $K_c = 3N_c kT_c/2$ for a number of particles $N_c = M_c/(\mu_c m_H)$ in the core, and the gravitational potential energy of the core is $U_c \sim -3GM_c^2/(5R_c)$.

• The modification is that we no longer have a zero pressure boundary condition at the core/envelope interface (as opposed to the stellar surface), so we have an energy term $3P_cV_c$ appearing.

• We now solve for P_c, yielding

$$P_c = \frac{3}{4\pi R_c^3}\left(\frac{M_c kT}{\mu_c m_H} - \frac{GM_c^2}{5R_c}\right) \quad . \tag{20}$$

To provide maximal support in the red giant phase, for fixed core mass and temperature, we can differentiate w.r.t. R_c to yield

$$\frac{\partial P_c}{\partial R_c} = 0 \quad \Rightarrow \quad R_c \sim \frac{4}{15}\frac{GM_c\mu_c m_H}{kT_c} \quad . \tag{21}$$

Then the scaling

$$P_c \approx \frac{GM_c^2}{20\pi R_c^4} \sim 3GM_c^2\left(\frac{kT_c}{GM_c\mu_c m_H}\right)^4 \tag{22}$$

quickly follows. This can be equated to the pressure exerted by the overlying material in the envelope, which is the force per unit area, i.e.

$$P_e \;\sim\; \frac{GM^2}{R^4} \;\sim\; \frac{\rho_e}{\mu_e m_H}\, kT_c \quad . \tag{23}$$

The first equality is essentially the virial theorem applied to the envelope, with zero outer pressure. The second equality asserts that the equation of state in the envelope is set by the temperature at the core-envelope interface.

Setting $\rho_e = 3M/(4\pi R^3)$, we can solve for R to yield

$$P_e \;\sim\; GM^2 \left(\frac{kT_c}{GM\mu_e m_H} \right)^4 \tag{24}$$

This is identical to Eq. (22) but with $\mu_c \to \mu_e$ and $M_c \to M$. It follows that the solution of $P_e = P_c$ then generates the solution $M_c/M \sim (\mu_e/\mu_c)^2$.

• Note that detailed treatment of the coefficients and radial gradients beyond the 2-zone simplification is somewhat superfluous, since we have ignored quantum **electron degeneracy pressure**.

∗ This fermionic property spawned by the Pauli exclusion principle, provides a zero-point temperature-independent pressure that provides considerable contribution to the solar mass, subgiant phase.

• The importance of the **Schönberg-Chandrasekhar limit** is that it helps identify the end state of evolution of a particular star; low mass cores will probably end up as white dwarfs. This connects to the Vogt-Russell Theorem through the envelope/core metallicity ratio μ_e/μ_c .

10. STELLAR EVOLUTION II

Matthew Baring – Lecture Notes for ASTR 350, Fall 2021

1 Late Stages of Stellar Evolution

Later on in the evolution of a main sequence star, there is the appearance of multiple shells of thermonuclear burning of different isotopes, accompanied by intense convective behavior and extensive mass loss. Key elements of the evolutionary sequence can be summarized as follows.

C & O, Sec. 13.2

Plot: Post Main Sequence Stellar Evolution

• At the end of main sequence phase the core has evolved mostly to helium and shrinks. This heats the surrounding hydrogen shell, which ignites and pushes the star through the subgiant phase with expansion of the envelope.

∗ Once the Schönberg-Chandrasekhar limit is reached (locus point 5), the core collapses further on a (short) Kelvin-Helmholtz timescale $t_{\rm KH} \sim \Delta E_g/L \sim GM^2/(LR)$. The core is no longer approximately isothermal, and the hydrogen shell is heated and narrowed significantly.

∗ The increased energy generation is not converted into luminosity, but is absorbed by *envelope expansion*, with active convection penetrating down towards the core. The star moves to the red with a drop in luminosity and effective temperature with significant contribution from H^- to opacity.

∗ *This implies the existence of spectroscopic signatures of convective action,* distinguishing such stars from solar-type abundances.

Plot: Benchmark: Solar Abundances

Evolution of a Massive Star

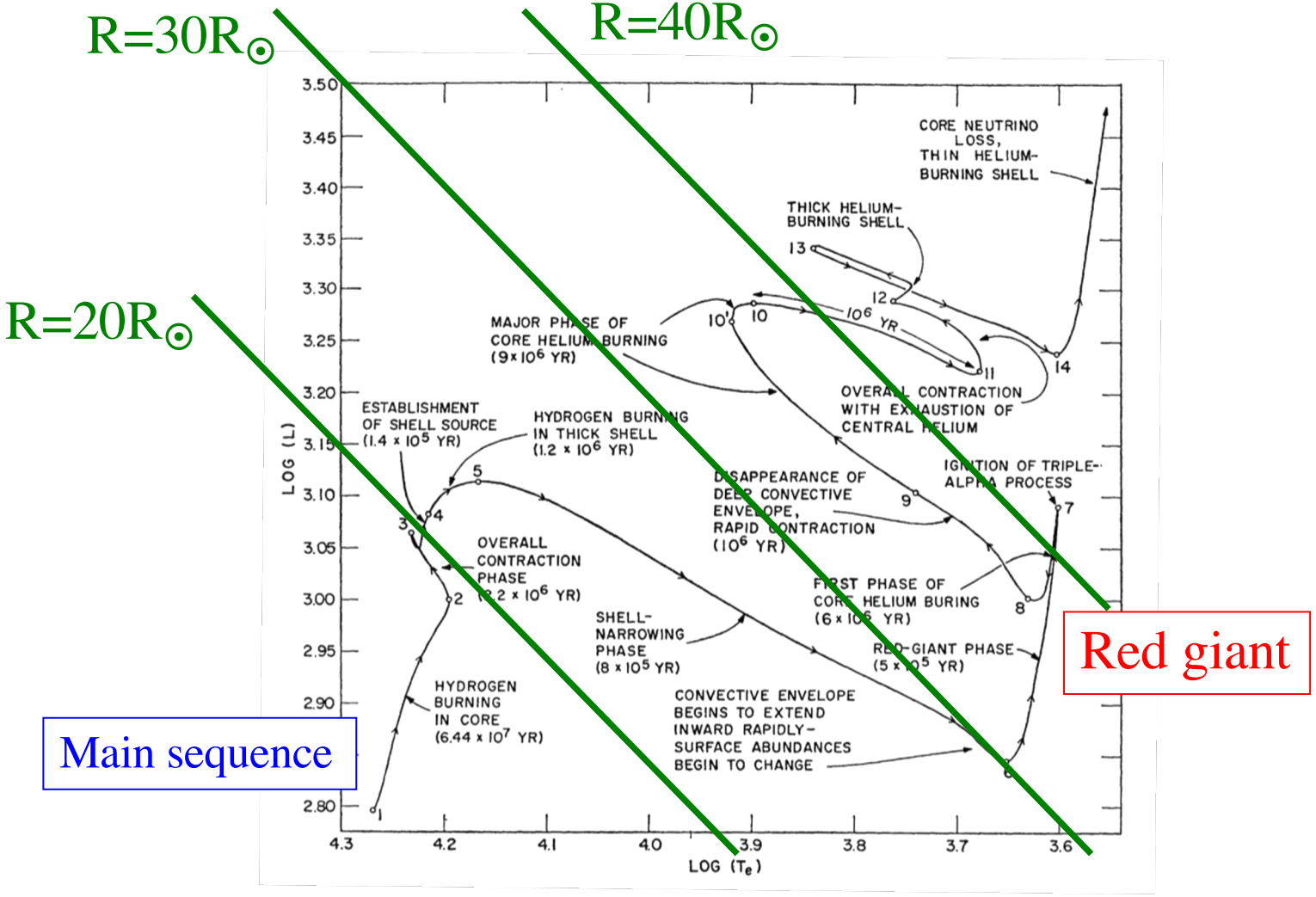

- Post main sequence evolution of a $5M_\odot$ star. Iben, I., ARAA **5**, 571 (1967).

Solar System Elemental Abundances

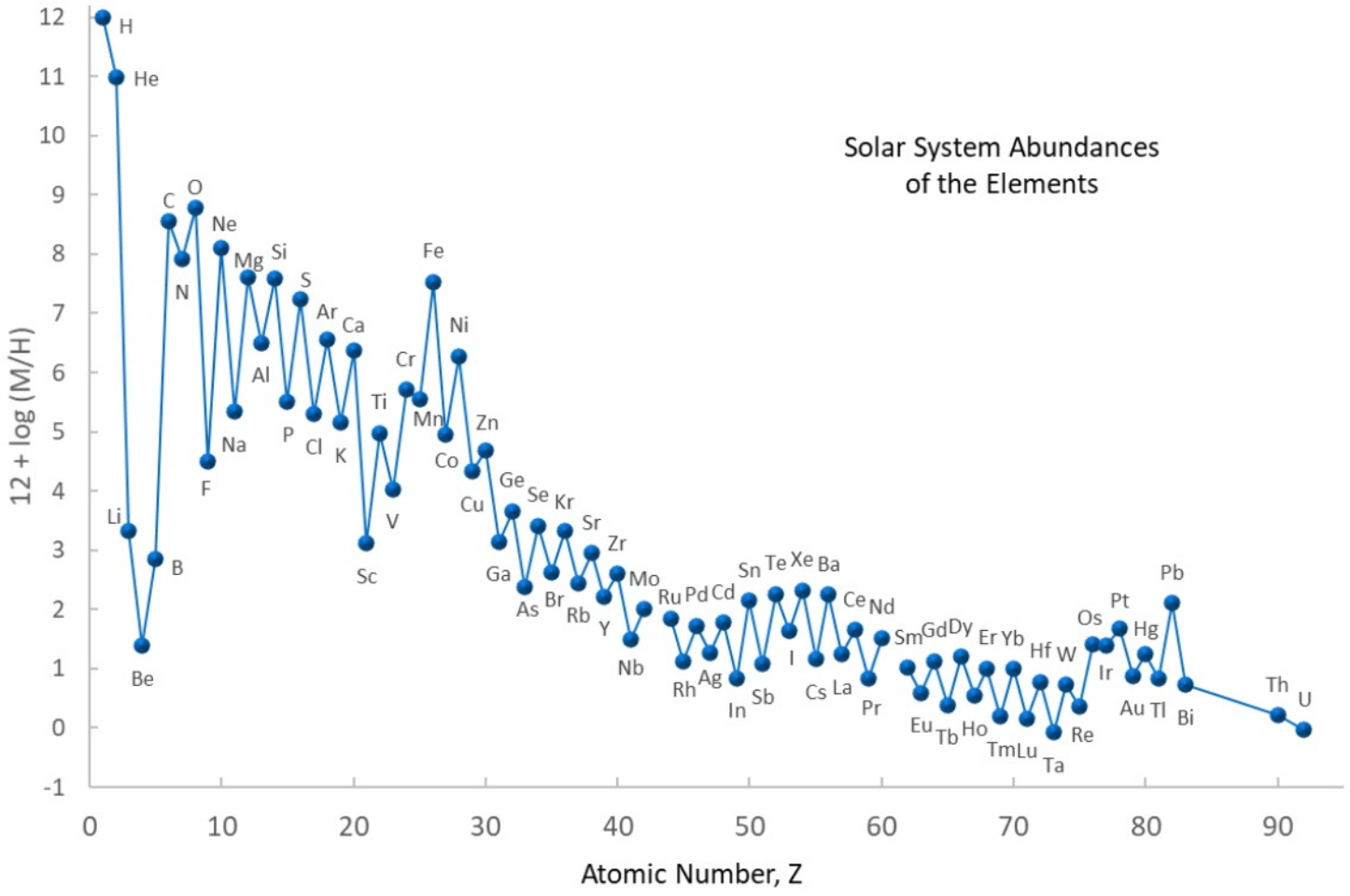

- From Lodders, K. 2020, Solar Elemental Abundances (Oxford University Press) [arXiv.org/1912.00844]